Virology 529 (2019) 195–204

Contents lists available at ScienceDirect

Virology

journal homepage: www.elsevier.com/locate/virology

Comparative study of chikungunya Virus-Like Particles and Pseudotyped-Particles used for serological detection of specific immunoglobulin M

Gérald Theillet[a,b], Jérôme Martinez[c], Christophe Steinbrugger[c], Dimitri Lavillette[d], Bruno Coutard[e], Nicolas Papageorgiou[e], Pascal Dalbon[a], Isabelle Leparc-Goffart[b,f], Frédéric Bedin[a,*]

[a] bioMérieux, Innovation New Immuno-Concepts, Chemin de l'Orme, 69280 Marcy-l'Etoile, France
[b] Unité des Virus Emergents (UVE: Aix-Marseille Univ. – IRD 190 – Inserm 1207 – IHU Méditerranée Infection), Marseille, France
[c] bioMérieux, R&D Immunoassays dpt., Biomolecule Engineering – bioMAP, Chemin de l'Orme, 69280 Marcy-l'Etoile, France
[d] Unit of Interspecies Transmission of Arboviruses and Antivirals, CAS Key Laboratory of Molecular Virology and Immunology, Institut Pasteur of Shanghai, Chinese Academy of Sciences, Shanghai, China
[e] Aix Marseille Université, CNRS, AFMB UMR 7257, Marseille, France
[f] IRBA, Unité de virologie - CNR des Arbovirus, HIA Laveran - CS50004, 13384 Marseille cedex, France

ARTICLE INFO

Keywords:
Virus-like particles
Pseudotyped virus
Field-flow fractionation
Arbovirus
Chikungunya

ABSTRACT

The incidence of chikungunya virus (CHIKV) infection has increased dramatically in recent decades. Effective diagnostic methods must be available to optimize patient management. IgM-capture Enzyme-Linked Immunosorbent Assay (MAC-ELISA) is routinely used for the detection of specific CHIKV IgM. This method requires inactivated CHIKV viral lysate (VL). The use of viral bioparticles such as Virus-Like Particles (VLPs) and Pseudotyped-Particles (PPs) could represent an alternative to VL.

Bioparticles performances were established by MAC-ELISA; physico-chemical characterizations were performed by field-flow fractionation (HF5) and confirmed by electron microscopy.

Non-purified PPs give a detection signal higher than for VL. Results suggested that the signal difference observed in MAC-ELISA was probably due to the intrinsic antigenic properties of particles.

The use of CHIKV bioparticles such as VLPs and PPs represents an attractive alternative to VL. Compared to VL and VLPs, non-purified PPs have proven to be more powerful antigens for specific IgM capture.

1. Introduction

The chikungunya virus (CHIKV) is an arbovirus (arthropod-borne virus) transmitted by infected *Aedes* mosquitoes (Furuya-Kanamori et al., 2016). Arboviruses are mainly prevalent in tropical and subtropical areas and represent a serious public health concern for developing countries (Burt et al., 2017). CHIKV belongs to the *Togaviridae* family (*Alphavirus* genus), which also contains Ross River, Mayaro, Semliki Forest and O'Nyong-Nyong viruses (Rathore et al., 2017). CHIKV was first isolated in Tanzania in 1952 (Lumsden, 1955; Robinson, 1955) and became endemic in large areas of Africa, the Middle East, India and Southeast Asia (Hammon et al., 1960; Rougeron et al., 2015). Between 2005 and 2007, CHIKV caused a massive epidemic on the island of La Réunion (Brouard et al., 2008). Since 2013, the rapid spread of the virus has been reported in the Caribbean and Central and South America. CHIK is an acute, highly symptomatic illness characterized by strong fever, headache, intense asthenia, rash, myalgia and severe arthralgia (Schwartz and Albert, 2010). Severe arthralgia that mainly affects hands, wrists, elbows, ankles and knees can evolve to chronicity. To date, there is no specific and efficient treatment.

In vitro diagnostic tests, based either on polymerase chain reaction (RT-PCR) or enzyme-linked immunosorbent assay (ELISA) can provide sensitive results and help optimize patient care (Mishra et al., 2011, 2018).

For specific type M immunoglobulin (IgM) serological diagnostic, an IgM-capture Enzyme-Linked Immunosorbent Assay (MAC-ELISA) is traditionally performed using viral lysate as antigen (Martin et al.,

* Corresponding author.
E-mail addresses: gerald.theillet@biomerieux.com (G. Theillet), jerome.martinez@biomerieux.com (J. Martinez), christophe.steinbrugger@biomerieux.com (C. Steinbrugger), dlaville@ips.ac.cn (D. Lavillette), pascal.dalbon@biomerieux.com (P. Dalbon), frederic.bedin@biomerieux.com (F. Bedin).

https://doi.org/10.1016/j.virol.2019.01.027
Received 20 September 2018; Received in revised form 28 January 2019; Accepted 29 January 2019
Available online 30 January 2019

2000). Viral lysate leads to good sensitivity of detection, and is used in reference laboratories (Martin et al., 2000). However, obtaining viral lysate is time-consuming and requires that production be conducted in a Biosafety Level 3 laboratory by qualified persons (McFee, 2018). Moreover, before lysis, the virus must be inactivated using chemical treatment such as β-propiolactone (BPL) before use (Perrin and Morgeaux, 1995). BPL could alter the overall structure of viral envelope proteins, which could modulate the affinity of antibodies for these proteins and thus decrease the sensitivity of the test (Fan et al., 2017). Consequently, finding alternative antigens for CHIKV serological diagnosis may be important. Among these alternative antigens, recombinant proteins are noninfectious and can be produced in quantity. However, hitherto, their performance has meant that they are rarely used instead of viral lysate (Cho et al., 2008; Priya et al., 2014).

Virus-Like Particles (VLPs) and Pseudotyped-Particles (PPs) represent potential alternative antigens for CHIKV serological diagnosis. VLPs and PPs are noninfectious multiprotein structures and represent an important class of biomolecular particles composed of self-assembling viral proteins (Pattenden et al., 2005; Urakami et al., 2017). These particles have been used in many applications such as for bioluminescent imaging in a mouse model for the evaluation of vaccines and antiviral therapies against CHIKV (Wu et al., 2017), and for the development of new-generation vaccines. Indeed, VLPs evoke effective immune responses without triggering the side effects associated with the native virus (Noranate et al., 2014; Saraswat et al., 2016). Some vaccines based on VLPs or PPs have been developed (Conner et al., 1996; Kushnir et al., 2012; Urakami et al., 2017), for example for the Hepatitis B virus (Scolnick et al., 1984), the H5N1 influenza virus (Pushko et al., 2005), strains of the human papilloma virus (Koutsky et al., 2002) and the chikungunya virus (Chang et al., 2014; Metz et al., 2013; Saraswat et al., 2016; Schwameis et al., 2016). The use of PPs or VLPs in diagnostics, and more specifically for IgM or IgG serology, has not been the subject of much investigation (Li et al., 2014).

In the present paper, PPs and VLPs were compared to VL by MAC-ELISA. In order to better understand the performance differences observed in CHIKV MAC-ELISA for these two types of particles, comparative physico-chemical and immunological characterizations were performed.

2. Materials and methods

2.1. Materials and specimens

The anti-E2 monoclonal antibody (3E10A5) was internally produced by bioMérieux SA (Lyon, France). 3E10A5 was directed against a conformational epitope of E2. As needed, it can be labeled with alkaline phosphatase (AP) following conventional procedures. CHIKV VLPs and PPs were produced in the *Laboratoire d'infectiologie virale et de pathologie comparée*, UMR754, of the *Institut National de la Recherche Agronomique* (INRA, Université Claude Bernard, Lyon, France). The CHIK viral lysate (VL) was produced and purified by the *Centre national de reference des arbovirus* (CNR Arbovirus, *Institut de Recherche Biomédicale des Armées*/IRBA, Marseille, France) using standard procedures (Martin et al., 2000; Yap et al., 2010). CHIKV capsid recombinant protein was ordered from Immune Technology (New York, NY, USA), and CHIKV envelope proteins (E1 and E2) were ordered from Aalto Bio Reagents (Dublin, Ireland).

CHIKV-negative sera and whole blood specimens were obtained from healthy donors from the French National Blood Bank (*Etablissement Français du Sang*, Lyon, France). Patient serum specimens were obtained from Biomnis, ABO (Lyon, France) and IRBA (Marseille, France) through specific contracts with bioMérieux SA. Informed consent was obtained for any experimentation. All experiments were performed in compliance with relevant laws and institutional guidelines and in accordance with the ethical standards of the Declaration of Helsinki.

2.2. VLPs and PPs production and purification

The method was inspired by previous studies (Metz and Pijlman, 2016; Noranate et al., 2014). Briefly, for the PPs, 293 T eukaryotic cells (ICAAC, Washington, USA) were co-transfected with the pTG5349 murine leukemia virus (MLV) packaging plasmid, the pTG13077 plasmid, encoding an MLV based vector containing a CMV-GFP internal transcriptional unit (kindly provided by Transgene Strasbourg, France) and a plasmids encoding the Gag-Pol (core) proteins of Murine leukemia virus, the Green Fluorescent Protein (GFP) or the chikungunya La Réunion infectious clone (LRic strain LR2006 OPY1) viral envelope glycoproteins (the last 35 Capsid amino acids in frame with E3, E2, 6 K and E1 under a CMV promoter), by the CaCl2 method (Clontech transfection kit, Clontech, Fremont, Ca, USA) following the manufacturer's instructions. After transfection, the cells were incubated overnight at 37 °C. The transfection was checked on the next day by monitoring the presence of GFP in the cells using a flow cytometer (FACS Calibur, Becton-Dickinson, Franklin Lakes, NJ, USA). For VLPs, the same protocol was applied except that only one plasmid, containing the genes encoding the different structural proteins of the CHIKV (Capsid, E3, E2, 6 K and E1, under a CMV promoter), was used. After an additional 24 h of incubation, the cell culture medium containing the unpurified VLPs or PPs (u-VLPs or u-PPs) was harvested and filtered using a 0.45 μM filtration unit (Merck-Millipore, Burlington, MA, USA).

The filtered cell culture medium was either frozen at −30 °C or purified by ultracentrifugation. In the latter case, the medium was loaded on a 2 mL sucrose cushion (20% W/V in PBS1x) and ultracentrifuged at 107,000*g* for 2 h at 4 °C (SW 41 T rotor, Beckmann Optima LE 80 K ultracentrifuge, Indianapolis, ID, USA). The pellet containing the particles was resuspended in PBS1x and then frozen and stored at −30 °C.

For a 10 cm Petri dish (containing 7 mL of DMEM medium supplemented with 10% of fetal bovine serum – DMEMc –, Invitrogen, Carlsbad, CA, USA), about 60 μL of purified VLPs (p-VLPs) or purified PPs (p-PPs) were recovered.

2.3. MAC-ELISA

The IgM antibody capture ELISA proceeded according to standardized methodology (Khan et al., 2014; Martin et al., 2000; Peyrefitte et al., 2005). In brief, polystyrene 96-well plates were coated overnight at 4 °C with 5 μg mL^{-1} of goat anti-human IgM (Jackson ImmunoResearch, Baltimore Pike, PS, USA) in PBS1x. Plates were washed with PBS1x containing 0.05% Tween-20 and blocked with a solution of PBS1x −0.5% BSA for 1 h at 37 °C. Fifty microliters of patient serum at 1:200 dilution were added and incubated for 1 h at 37 °C. Fifty microliters of CHIKV antigens at 1:400 dilution in PBS1x were then added and incubated for 2 h at 37 °C. The optimal antigen concentration was experimentally determined for each antigen: u-VLPs or u-PPs were used undiluted and the viral lysate inactivated by BPL was used at 1:400 dilution. Purified PPs (p-PPs) were used at 1:20 dilution. Finally, 0.5 μg mL^{-1} of AP-conjugated anti-E2 monoclonal antibody (3E10A5, bioMérieux SA) was added into each well and incubated for 1 h at 37 °C. After intensive washing, the reaction was carried out at room temperature for 15 min after addition of a PNPP solution (P-NitroPhenyl Phosphate, ThermoFisher Scientific, Hillsboro, OR, USA) and was stopped by adding 2 N sodium hydroxide. The optical density (OD) was measured at 450 nm in a plate reader (Eon Biotek, Biotek Instruments, Winooski, VT, USA).

2.4. Hollow-fiber flow field-flow fractionation (HF5) with multiple-angle light scattering (MALS)

Studies were based on previous experiments, using HF5 and MALS detection (Pease et al., 2009; Wagner et al., 2014; Yohannes et al., 2011). HF5-MALS-UV-dRI analysis was conducted using the Eclipse

Dualtec separation system device (Wyatt Technology Europe, Dernbach, Germany), coupled with a ThermoFisher/Dionex Ultimate 3000 RS pump, a DAD-3000 Ultraviolet (UV)/visible photodiode array detector (ThermoFisher Scientific), a Heleos Dawn 8 + MALS detector (Wyatt Technology Corporation, Santa Barbara, CA, USA) and an Optilab T-rEX differential Refractive Index (dRI) detector (Wyatt Technology Corporation). The separation device consisted of a hollow-fiber 400 µm radius with a 10 kDa cut-off PES membrane and a 90 µL channel volume. All operations were conducted using phosphate saline buffer (7 mM PO4, 150 mM NaCl, pH 7.2).

For each analysis run, 1 min of elution and 1 min of focus were carried out on the system at the beginning of the experiment. Then, the HF5 system was maintained in "Focus + Inject" mode for the next 6 min, with buffer injected into the channel from both the inlet and outlet points at 0.45 mL min^{-1}. A volume of 20 µL of undiluted VLPs and PPs samples were injected into the channel during this time. Then, the system was switched to "Elution + Cross-flow mode", with flow through the channel set to 0.5 mL min^{-1} for 10 min. Finally, during the "Elution – Cross-flow" step, the elution was maintained but the cross-flow was decreased to 0.03 mL min^{-1} for 5 min and maintained at 0.03 mL min^{-1} for 20 min.

Eluant was passed through a sequence of UV absorbance, MALS and dRI detectors for concentration and size analysis. UV was monitored at 280 nm with a ThermoFisher/Dionex DAD-3000 detector. For the purposes of this study, the UV extinction coefficient (ε) for all proteins was assumed to be 1.1 mL mg^{-1} cm^{-1} (theoretical value calculated from the amino acid sequences of CHIKV envelope and capsid proteins) and the differential refractive index (dn/dc) for all proteins was assumed to be constant at 0.185 mL g^{-1} for all refractive index signals (Huglin MB, 1972). The root mean square geometric radius of eluted particles was determined using a MALS detector. Anisotropic light scattering signals for particles used a "sphere" regression in ASTRA 7 software, assuming that all encountered particles were VLPs or PPs and were perfectly spherical. In the case of non-spherical regression, the size was expressed in rms (root mean square) radius. For the VLPs or PPs peaks, the methods developed by Zimm, Berry and Debye were applied to both the 1st and 2nd order (Andersson et al., 2003). All these models fit to a $R^2 > 0.99$. However, to allow the counting of particle number density, the spherical regression model was selected.

2.5. Electron microscopy

Purified VLPs and PPs were analyzed using electron microscopy and 2D image processing (Baklouti et al., 2017). Samples were diluted to 0.05 mg mL^{-1}, and a 4 µL drop was applied to a glow-discharged formvar-carbon-coated grid (Copper 300, Polysciences Inc. Warrington, PA, USA). After 45 s of incubation, the grid was stained (2% uranyl acetate) with Nano-W® (Nanoprobes Inc., Yaphank, NY, USA) and transferred into a FEI Tecnai Spirit G2 electron microscope (Thermo Fisher, Hillsboro, OR, USA) operated at 120 kV. 270 images were recorded with an EAGLE 2kX2k CCD camera (Raptor Photonics, Larne, Northern Ireland) with a range of 1.5–2.2 µm under focus.

2.6. Avidity ELISA

For avidity ELISA, the steps until the addition of the antigens are identical to the MAC-ELISA protocol (Martin et al., 2000). Then, 50 µL of solutions of various molarity (from 0.5 M to 3 M) of urea (Sigma, Saint-Louis, MI, USA) were added and incubated for 15 min at room temperature. After intensive washing, 0.5 µg mL^{-1} of AP-conjugated anti-E2 monoclonal antibody (3E10A5, bioMérieux SA) was added into each well and incubated for 1 h at 37 °C. After washing, the reaction was carried out at room temperature for 15 min after addition of a PNPP solution (P-NitroPhenyl Phosphate, ThermoFisher Scientific) and stopped by adding 2 N sodium hydroxide. The optical density (OD) was measured at 450 nm in a plate reader (Eon Biotek, Biotek Instruments, Winooski, VT, USA).

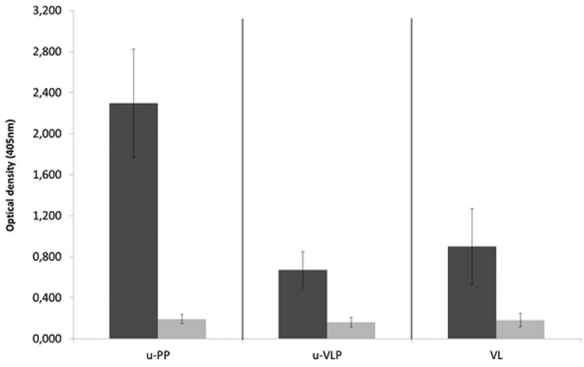

Fig. 1. CHIKV IgM detection by MAC-ELISA using different CHIKV antigens. Black bars: test; gray bars: negative control using healthy patient serum (no CHIKV IgM). Each condition has been conducted twenty folds in duplicate. u-PPs / u-VLPs: unpurified PPs/VLPs; VL: viral lysate.

3. Results

3.1. CHIKV IgM detection by MAC-ELISA

In order to find an alternative antigen to VL, which is usually used in CHIKV MAC-ELISA, a variety of other antigens, including CHIKV PPs and CHIKV VLPs, were assessed.

The VLPs/PPs purification steps (i.e. centrifugation; see Materials and Methods) were time-consuming and resulted in a significant loss of material. It has previously been demonstrated that unpurified PPs gave an enhanced signal compared to other alternative antigens, including the purified PPs. No cross-reactivity was noticed with alphaviruses samples other than CHIKV or flaviviruses samples (unpublished results). When VLPs and PPs were tested unpurified (u-PPs and u-VLPs), the cell culture supernatant containing the VLPs/PPs was used directly. Samples from healthy patients (without CHIKV IgM) were used as negative control.

As illustrated in Fig. 1, for experiments conducted on twenty CHIKV-IgM-positive patient sera tested in duplicate, a strong signal was observed for a MAC-ELISA using u-PPs (OD = 2.298 ± 0.525). The signal was approximately 2.6 times higher than for viral lysate (OD = 0.900 ± 0.369), which was considered as the reference assay. The non-purified VLPs, u-VLPs, presented a signal 1.34 times lower than the signal observed for the VL, and 3.4 times lower than for the u-PPs.

The results confirmed that, among the variety of antigens tested by MAC-ELISA, the CHIKV u-PPs gave the highest signal intensity for specific CHIK IgM detection and can be used as an alternative antigen to VL in MAC-ELISA. VLPs can also be used but the signal intensity was close to that obtained for VL.

3.2. Impact of cell culture medium associated with PP on MAC-ELISA

In order to confirm that the signal associated with unpurified PPs was only due to the presence of PPs and not to viral proteins released in the cell culture supernatant, and to study the impact of the DMEMc medium on the signal, MAC-ELISAs were performed on purified PPs resuspended in PBS1x, and then diluted either (i) in PBS1x, (ii) in fresh, non-ultracentrifuged DMEMc medium, or (iii) in the cell culture supernatant (DMEMc) after ultracentrifugation (Fig. 2a). Particles were diluted 1:116. Each condition was studied on two specific CHIKV-IgM-positive human sera in duplicate, and on two healthy (CHIKV-negative) patient sera.

The results (Fig. 2b) indicated that purified PPs, diluted in either ultracentrifuged DMEMc or fresh non-ultracentrifuged DMEMc, had a

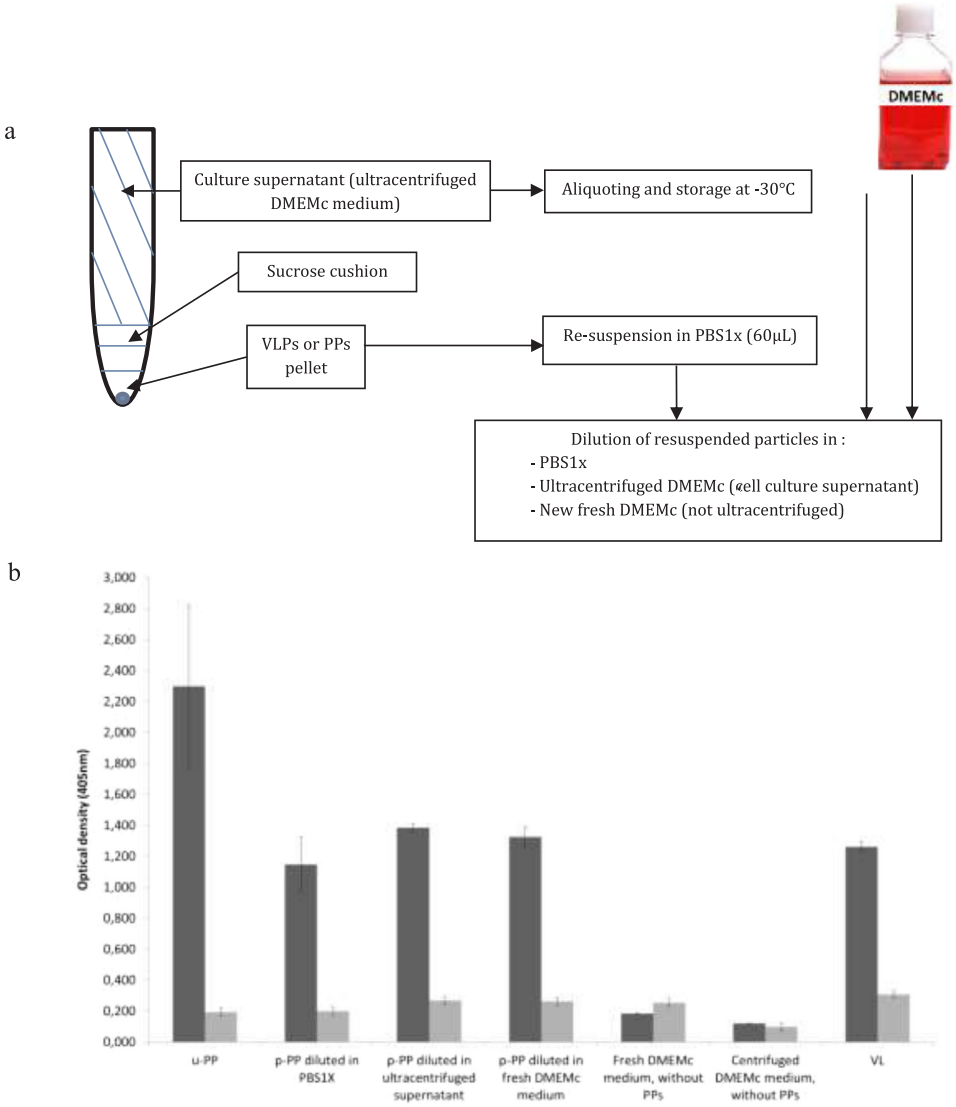

Fig. 2. MAC-ELISA with purified PPs resuspended in cell culture DMEMc medium or in fresh DMEMc. a) flowchart of the experiment. b) CHIKV IgM MAC-ELISA using purified PPs resuspended in different buffer. u-PPs: unpurified PPs; p-PPs: purified PPs; VL: viral lysate. Black bars: test; gray bars: negative control using healthy patient serum (no CHIKV IgM).

signal close to that of the Gold Standard using VL (OD = 1.384 ± 0.026, OD = 1.323 ± 0.063 and OD = 1.259 ± 0.033, respectively). The signals corresponding to the conditions where p-PPs were diluted in DMEMc medium were approximately 1.18 times higher than the signal obtained with p-PPs diluted in PBS1x (OD = 1.145 ± 0.177). Moreover, samples tested with p-PPs diluted in PBS1x remained 2 times lower than u-PPs (OD = 1.145 ± 0.199 and OD = 2.298 ± 0.525, respectively).

These results confirmed that the strong signal obtained with u-PPs was not linked to the cell culture medium or the presence of residual proteins but was mainly associated with the presence of PPs. Moreover, PP purification by ultracentrifugation seemed to impact on the MAC-ELISA signal.

3.3. HF5-MALS-UV-DRI characterization of CHIKV VLPs and PPs

In order to compare the size, morphology, and purity of VLPs and PPs, HF5-MALS-UV-dRI technology was deployed.

The first analyses were conducted on unpurified VLPs/PPs. However, the results obtained had a high level of background noise due to the presence of proteins from DMEMc and cell debris and were uninterpretable. In consequence, HF5-MALS analyses were performed on purified CHIKV particles.

The most probable hypothesis was that the VLPs and PPs were spheres, so we used a spherical regression model applied to p-VLPs and p-PPs in order to reduce the background noise generated by components of the culture medium (DMEMc). The signals obtained for VLPs (Fig. 3a) and PPs (Fig. 3b) were of good quality (fit R^2 = 0.9904 for the VLPs data and fit R^2 = 0.9998 for the PPs data) with small calculation errors in the numerical value results. VLPs and PPs were detected from about 22 min to approximately 45 min after injection. Contaminants were detected between 8 and 16 min after the beginning of the experiment, both for VLPs and PPs conditions. The hypothesis was that these contaminants were proteins from cell debris or culture medium that were not completely removed during the ultracentrifugation step.

The VLPs/PPs concentration was determined from a $UV_{280\,nm}$ reading. The size of the bioparticles was determined by light scattering (MALS monitor).

Considering all bioparticles analyzed between 25 and 45 min, the concentration for the VLPs was estimated as 0.75 µg for 20 µL injected (3.6×10^7 particles mL^{-1}). A large size range was observed, indicating polydispersity (or clusters of two or more particles). The particles had a

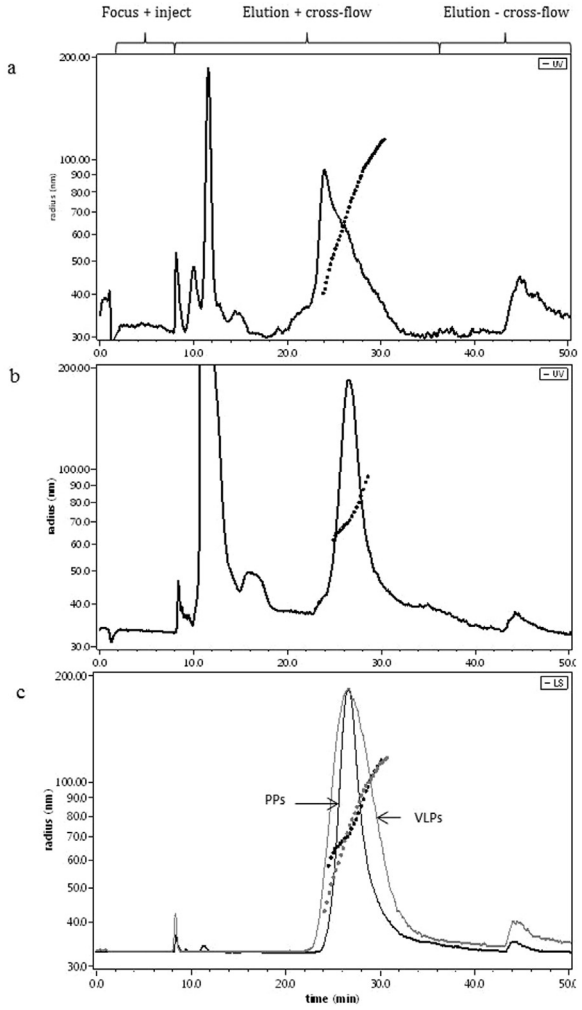

Fig. 3. Fractograms of CHIKV particles read on HF5-UV$_{280\,nm}$-MALS. a) purified VLPs; b) purified PPs. The fractograms show the particles separation by HF5-MALS over time, obtained with the UV photodiode array detector. The black dots curve represents the size distribution of the particles in each sample, obtained with the Multi-Angle Light Scattering (MALS) detector. c) Fractograms of CHIKV particles read on HF5-MALS. The fractograms show the particles separation by HF5-MALS over time, obtained with the Light Scattering (LS) monitor. The black dots curves represent the size distribution of the particles in each sample, obtained with the Multi-Angle Light Scattering (MALS) detector. Dark curves and dots: PPs. Gray curve and dots: VLPs.

geometric radius between 40 nm and 120 nm (see dotted curves in Fig. 3a and c) with an average radius of 73.3 nm (± 0.1%), corresponding to particle sizes of 80–240 nm in diameter.

Purified PPs were also analyzed and were shown to have similar characteristics to VLPs. They were polydispersed, with a geometric radius between 50 nm and 120 nm (see black dotted curves in Fig. 3b and c), with an average radius of 75.1 nm) ± 0.7%), corresponding to particle sizes between 100 and 240 nm in diameter. The concentration was estimated as 3.45 µg of PPs in the 20 µL analyzed (7.5×10^7 particles mL^{-1}).

Light scattering showed that both VLPs and PPs were detected at the same time after sample injection (Fig. 3c). However, the curve representing the VLPs (gray curve) was more spread out over time than the PPs curve, indicating a greater polydispersion of VLPs compared to PPs, as confirmed by the largest size scale observed for VLPs (gray dotted curve).

In order to check the extent to which the preparations were contaminated with free viral proteins or proteins from the culture medium, and to compare the profiles obtained on these proteins with those obtained on VLPs and PPs, recombinant proteins (proteins E1, E2 and C, see Fig. 4) were also analyzed in parallel by UV$_{280\,nm}$ absorbance. Each protein was concentrated at 1 µg mL^{-1} and 20 µL of each protein were analyzed. Pure Calf Serum Albumin (CSA) was also tested. Each protein was investigated in the same conditions as the CHIKV particles.

The analysis of the CSA showed a single peak, observed at approximately 11 min after injection. The same peak was observed in both VLPs and PPs profiles (Fig. 3 and Fig. 4), indicating that the CSA protein was not totally removed from the particle preparations by ultracentrifugation. In parallel, the recombinant proteins of CHIKV were quite distinct, and appeared between 8 and 14 min, upstream of the particle peaks (Fig. 4). Several peaks were observed for the E1 and E2 protein profiles. Because the poor quality of the data obtained, a molecular weight analysis could be performed only on two peaks. One of these peaks observed in VLPs profile was found to be 110 kDa and could correspond to dimers of Envelope protein. Another peak of 65 kDa observed on PPs profile could correspond to the BSA (60 kDa) or to monomers of CHIKV Envelope protein (55 kDa). Further characterization would be necessary to identify exactly the nature of the proteins corresponding to these peaks. All the results presented here were obtained repeatedly (more than twice).

Finally, a conformational plot (see Fig. 5) indicated that two morphologically different populations existed for each type of bioparticle. Particle morphology can be evaluated using the value of the slope of each regression curve. When the slope value is around 0.33, particles are considered spherical and homogenous in density. When the slope is around 0.5–0.6, particles are a random coil, and when the slope value is approximately 1.0 or more, particles form rods (Podzimek, 2011). The molecular weight range calculated for spherical PPs (2.10^7 to 6.10^7 g mol^{-1}) was narrower than for VLPs (10^7 to 6.10^7 g mol^{-1}), for a similar size range. According to the literature (Podzimek, 2011), a slope value of 0.33 corresponds to spherical particles, homogeneous in density. For a value smaller than 0.33, the core of the particles is denser than the outside. Viral bioparticles are synthesized in eukaryotic cells and can encapsulate various biomolecules during their biosynthesis and assembling. They also contain a viral capsid. All these elements make that these bioparticles have a denser core and are not homogeneous spheres. The comparison of the slope values suggested that VLPs were denser than PPs (slope value 0.18 for VLPs; 0.22 for PPs). In conclusion, purified VLPs or PPs preparations consisted essentially of whole particles, spheres and also rods (PPs) and random coils (VLPs), with few contaminant viral proteins. Residual CSA, originating from fetal calf serum used in cell culture medium, was possibly present.

3.4. Electron microscopy

In order to confirm observations made on HF5-MALS and perform direct observation of the particles, purified CHIKV VLPs and PPs were observed by transmission electron microscopy (TEM). These experiments could help confirm the previous results regarding production purity, morphology, size heterogeneity, and polydispersion of the particles (whether alone or clustered).

With regard to VLPs, TEM pictures showed a large heterogeneity in terms of the size and morphology of the particles (see Fig. 6). Indeed, spherical or partially spherical particles of various diameters (30–150 nm) were observed, confirming a large size heterogeneity. Moreover, particles were often clustered by 2 or 3, sometimes forming rod-shaped, non-spherical particles (see Fig. 6, black arrow). No major contaminants such as actin or protein filaments were found, indicating a high purity of the preparations.

With regard to PPs, spherical particles larger than VLPs were observed, with a diameter between 50 and 200 nm, showing greater heterogeneity in terms of size. PPs rarely seemed to be clustered and remained more often as single particles. However, due to poor purification (presence of actin filaments) the pictures were more difficult to

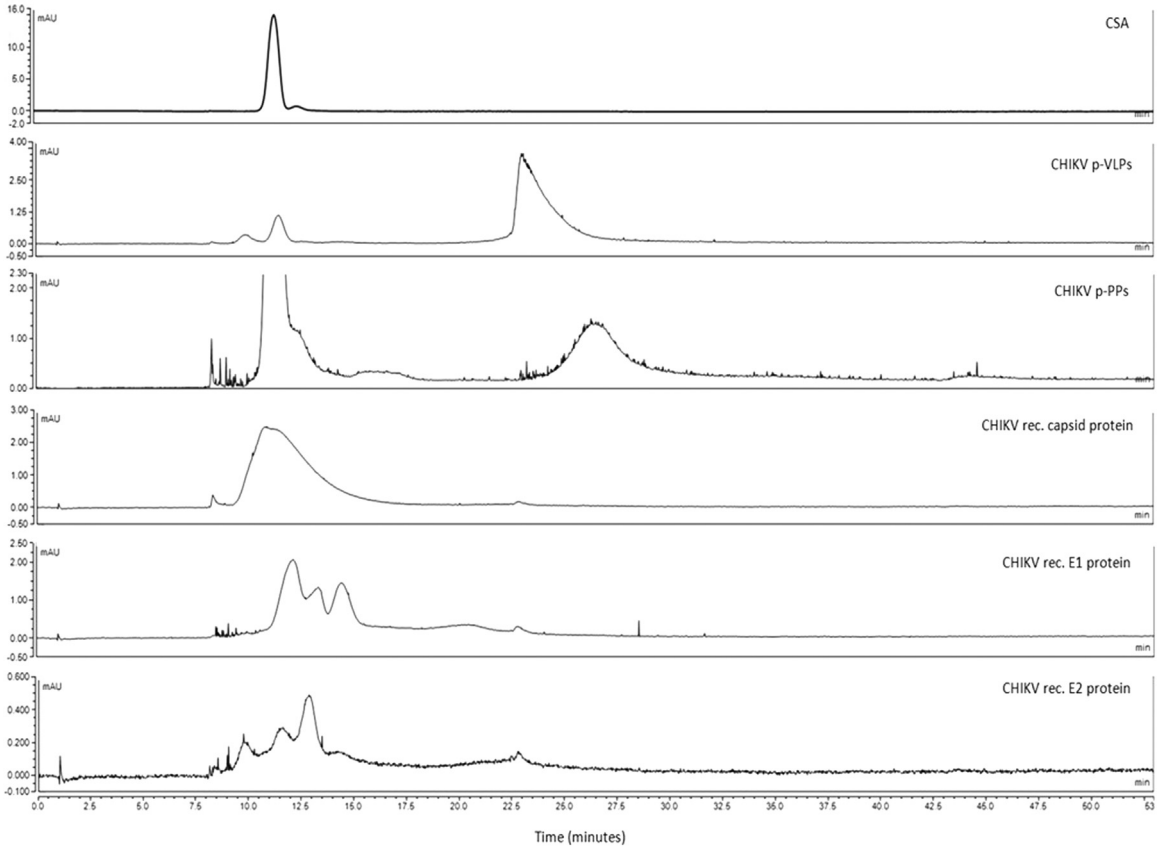

Fig. 4. Compilation of HF5-UV$_{280\,nm}$ graphs of CSA, VLPs/PPs and chikungunya antigens. CSA: Calf serum albumin; CHIKV p-VLPs: chikungunya virus purified Virus-Like Particles; CHIKV p-PPs: chikungunya virus purified Pseudo-Particles; rec E1: CHIKV Envelop 1 recombinant protein; E2: CHIKV Envelop 2 recombinant protein.

interpret than the VLPs pictures. (see Supplementary data 1, white arrows).

3.5. Avidity ELISA

The strong signal difference observed between MAC-ELISAs conducted with PPs or VLPs could be due to a difference in the presentation of the viral proteins at the surface of the viral particles, and therefore to their accessibility with regard to the E2 antibody or the specific human IgM.

In order to compare the strength of interactions between CHIKV specific IgM and VLPs or PPs, an avidity ELISA was performed (Fig. 7), inspired by previous studies (Gonzaga et al., 2011; Smolander et al., 2010). After a capture step of the specific antibodies, a progressive increase in urea molarity was used to progressively remove low avidity antibodies from antigen-antibody complexes (Aguado-Martinez et al., 2005). Indeed, urea is a chaotropic agent traditionally used for removing low avidity antibodies. For each molarity of urea, an Avidity Index (AI) was calculated using the following formula: AI = (OD with dissociating agent / OD without dissociating agent) *100 (%). The avidity ELISA was assessed on 6 different CHIKV sera (with high titers of specific IgM), in triplicate.

For PPs, from 0.5 M to 1.5 M of urea, the OD signal intensity remained relatively stable (between 94.2% and 96.5% AI) but decreased to 87.3% at 2 M of urea and 73.9% at 2.5 M of urea. The equation of the regression curve was y = -11.601x + 106.64. For VLPs, the OD signal intensity remained relatively stable from 0.5 M to 1 M of urea (between 100.503% and 101.614% AI) but decreased to 91.7% at 1.5 M of urea, reaching 73.2% at 2.5 M of urea. The linearization function of the various points of the curve was y = -14.43x + 112.1.

For VLPs, the correlation coefficient, a measure of the quality of the prediction of the regression line connecting each urea molarity point, was R^2 = 0.9416. In comparison, the same correlation coefficient for PPs was R^2 = 0.7863. For VLPs, and for PPs to a lesser extent, the regression equations suitably described the points distribution.

The slope of the VLPs curve (-14.43) was higher than for the PPs curve (-11.601), resulting in an earlier dropout of VLPs for IgM of interest than that of PPs for the same antibodies. CHIKV IgM potentially had higher affinity for PPs than for VLPs.

4. Discussion

Because of their ease of production and use (no purification step needed), unpurified bioparticles (u-VLPs and u-PPs) were used in the MAC-ELISA format, and the first observation was that the signal detected using u-VLPs was not significantly different from that obtained with VL. Consequently, u-VLPs can be used as an alternative antigen to VL in MAC-ELISA. Interestingly, u-PPs presented a significantly stronger signal detection, approximately 2–3 times higher than the other antigens (u-VLPs and VL). PPs seemed to be a better candidate for CHIK MAC-ELISA than VL. The signal observed in MAC-ELISA with u-PPs was not due to a difference in viral E2 protein concentration, as previously demonstrated by a Western Blot using the anti-E2 monoclonal antibody 3E10A5 used in MAC-ELISA (unpublished results).

Then, to better understand the signal difference observed between these bioparticles, further characterizations were performed.

The MAC-ELISA used unpurified VLPs and PPs as antigens, despite the fact that these particles are generally used purified after an ultracentrifugation step (Fontana et al., 2016; Lamounier et al., 2015; Li et al., 2014; Peyret, 2015). However, results obtained with purified

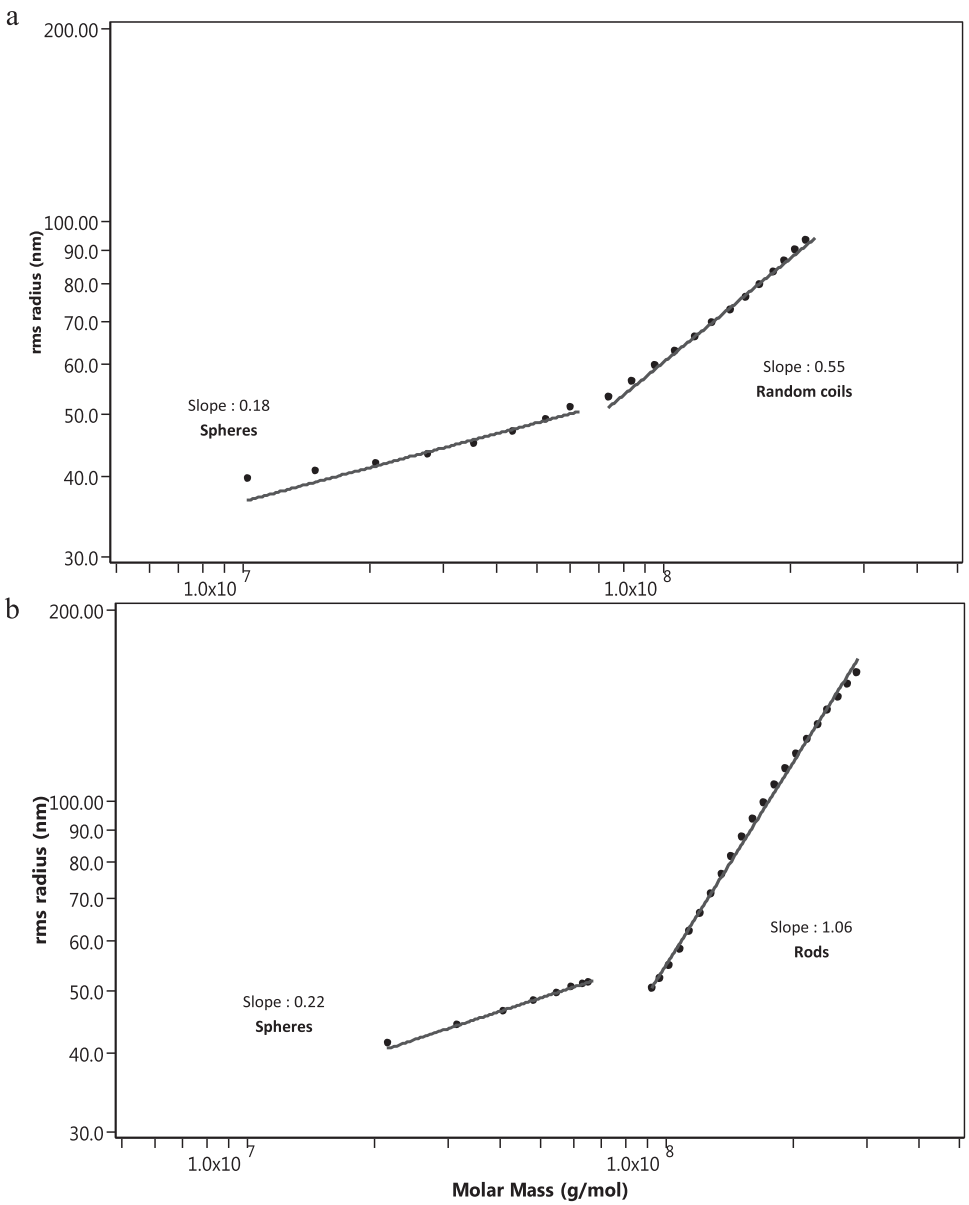

Fig. 5. Conformational plots of purified VLPs (a) and purified PPs (b) obtained by absorbance analysis ($UV_{280\,nm}$), representing the log10 of rms radius of the bioparticles as a function of the log10 of their molar mass (MM). Morphology of the particles can be deducted from the value of the slope of each regression curve.

particles showed results comparable to VL in CHIK MAC-ELISA. Unpurified PPs generated a significantly stronger signal than VL or purified particles. It was suggested that one of the components of the DMEMc medium in which the particles were present would promote the binding of specific CHIKV IgM, and thus increase the detection signal in comparison to other antigens. However, compared to p-VLPs, no signal increase was observed for u-VLPs, invalidating this assumption. Alternatively, the production of PPs could lead to the release of viral components in culture supernatant that could enhance the signal. However, when purified PPs (p-PPs) were diluted either in fresh DMEMc medium or in clarified cell culture supernatant, and tested in MAC-ELISA, the signal was very close to that obtained with the MAC-ELISA using p-PPs, indicating that components of the cell culture medium, including released viral components, were not involved, or only involved to a small extent, in the signal increase. It cannot be excluded that direct consequences of the purification step by ultracentrifugation are structural modifications of the particles that would impact on antigen presentation (Minder et al., 2011). These modifications could have an impact on particle conformation, infectivity, and antigenicity (Drake et al., 2010), indicating that the observed signal difference would be due to the intrinsic properties of particles. However, no signal difference was observed between u-VLPs and p-VLPs when tested by MAC-ELISA. Drake, Keswani et al. showed that proteins of serum contained in culture medium could have an impact on VLPs formation and infectivity activity, and that particles produced in culture media without serum (e.g. Opti-MEM®, Invitrogen) were significantly more efficient than those produced in culture media with serum (Drake et al., 2010). CHIKV VLPs and PPs have also been produced in Opti-Mem®, but no improved performance was observed compared to particles produced in DMEMc.

In order to more precisely characterize these bioparticles, additional analyses were performed on purified VLPs and PPs. Bioparticle recovery in the cell culture medium involved the presence of cell debris, in addition to the components of the cell culture medium. This meant that physical analyses of the bioparticles required separation of VLPs or PPs from the other components (cell debris, etc). A reliable advanced analytical tool was therefore needed to control the process and to assure the quality of the final product. The gentle separation mechanism of HF5, by which the structure and conformation of analytes is preserved,

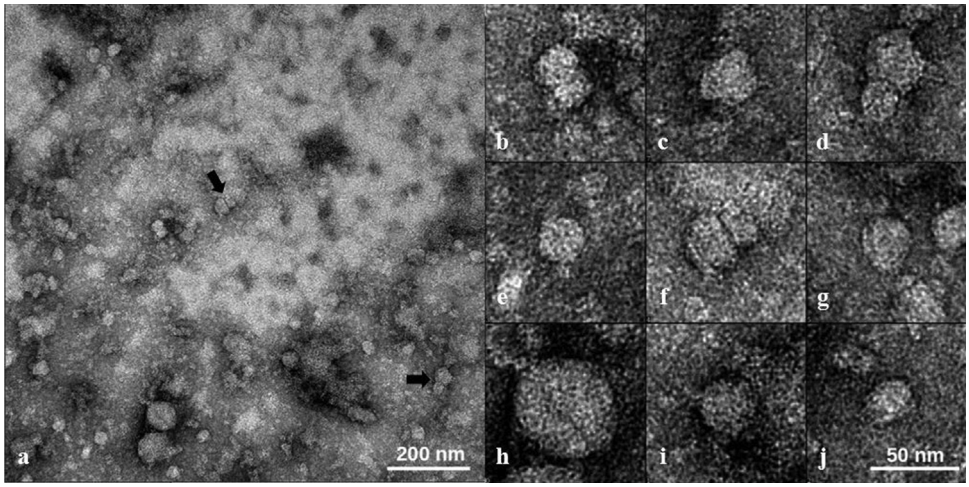

Fig. 6. CHIKV purified VLPs observed by Transmission Electron Microscopy. Black arrows: coupled CHIKV VLPs. a) low magnification picture; b to j) high magnification pictures.

makes it a very valuable technique for the precise characterization of VLPs and PPs (Yohannes et al., 2011).

HF5 detects spherical particles with a large size range (between 80 nm and 240 nm in diameter for VLPs and 100–240 nm in diameter for PPs), with polydispersion, between 22 and 45 min after injection. The use of a spherical modeling with Astra 7 fits with $R^2 > 0.99$, indicating that the spherical hypothesis used was relevant. VLPs were more concentrated than PPs for the same analyzed volume, and fewer contaminants were detected, suggesting a more efficient ultracentrifugation process for VLPs. Contaminant proteins were detected upstream of the spherical particles, between 8 and 14 min after injection into the HF5. Calf serum albumin (CSA) could represent the majority of these contaminants because it was over-represented in DMEMc, the medium used for VLPs production. The weak UV signal did not impact on the accuracy of the radius calculations because the light scattering signals from MALS were still of good quality. However, a peak of particles was observed between 44 and 46 min for the PPs analysis.

The presence of CHIKV viral proteins could be due to a release of free viral proteins during the bioparticle production, in addition to the serum albumin from the cell culture medium. For CHIKV proteins analyzed by HF5, the presence of a series of peaks was interpreted as multimeric forms of the proteins (homo- or heterodimers). For instance, during virus replication in target cells, the E1 and E2 envelope glycoproteins are assembled to form E1-E2 heterodimers, which will be transported to the cell membrane to form the envelope of the new virus (Jose et al., 2009). This auto-assembling process could explain the peaks observed between 8 and 14 min of retention time on HF5-MALS fractograms (see Fig. 3 and Fig. 4). Moreover, no angular dependence was observed for these molecules, suggesting that it was not particles. Indeed, angular dependence starts to be observed at 30 nm for the Heleos Dawn 8 + MALS system (manufacturer's specifications). The analytes detected upstream of the bioparticle peak did not have angular dependence, indicating that bioparticles such as VLPs or PPs were not present, but proteins or large protein aggregates were. The largest bioparticles were fully eluted at 45 min when the crossflow was turned off.

To confirm the results obtained with HF5, transmission electron microscopy experiments were performed. Observations carried out on purified bioparticles confirmed the presence of spherical VLPs and PPs, with a large range of size and heterogeneity. While the PPs were almost all single and near-spherical, the VLPs often appeared clustered 2 by 2 or 3 by 3, and were not always spherical, indicating morphological alterations. Contradictory observations were made with the HF5-MALS

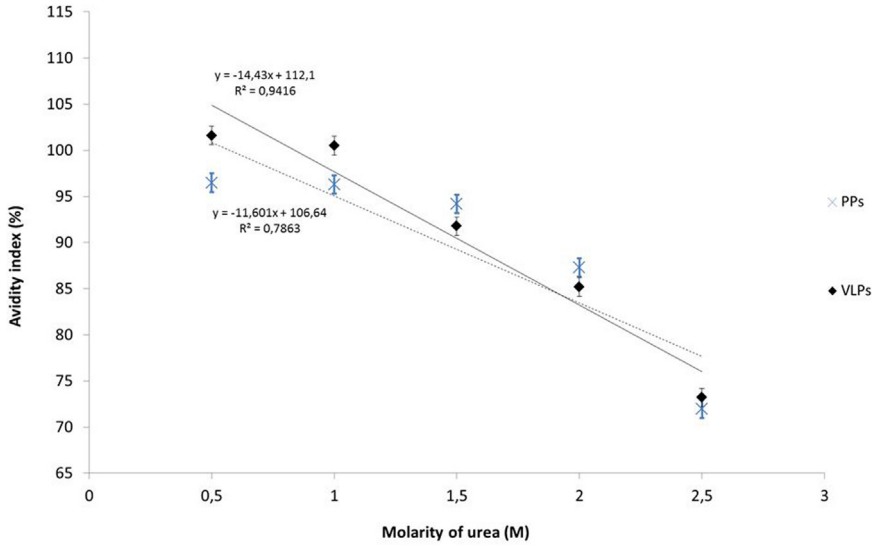

Fig. 7. Avidity ELISA on CHIKV p-PPs and p-VLPs. The experiment has been performed in triplicate on 6 different patient's samples. Black squares: p-PPs; X: p-VLPs.

analysis of the bioparticles. It was deduced that spherical bioparticles as well as elongated structures were present in our preparation. Elongated structures could actually correspond to spherical particles clustered 2 by 2 or even 3 by 3, as observed on MET. However, the slope value representing elongated structures made of PPs (1.06) is higher than the slope value for VLPs elongated structures (0.55). This would mean that there are more PPs elongated structures than VLPs elongated structures. However, previous MET observations showed that PPs were more often present as single particles, indicating that some elongated structures deduced from conformational plots could be protein contaminants such as actin filaments. HF5 is considered to be a more robust method than MET for the fine characterization of these bioparticles (Yohannes et al., 2011).

Several hypotheses concerning the morphological deformation of these particles have been issued. Pease, Lipin et al. assumed that structural deformation of bioparticles could be due to the absence of viral genome. Moreover, the deformations may also be the consequence of the fixing and staining methods used for electron microscopy (Pease et al., 2009). Furthermore, it has already been reported that the incorporation of foreign proteins into bioparticles, from cell culture or culture medium, causes deformations within VLPs structures, as observed for mouse polyomavirus VLPs production (Boura et al., 2005). Additionally, the purification steps (ultracentrifugation) could lead to morphological damage of particles. TEM observations for PPs were more difficult to read and understand because of the significant presence of contaminants from cell culture such as actin filaments. Fewer contaminants were observed for VLPs, which correlated with HF5-MALS observations, indicating that the purification step was more effective for VLPs than for PPs.

Studies concerning bioparticle characterization are rare (Qureshi and Kok, 2011). It has been shown that field-flow fractionation technology is able to quantitatively determine bioparticle size distributions with greater rapidity and statistical significance than TEM, providing useful technologies for product development and process analytics (Chuan et al., 2008; Pease et al., 2009).

All previous observations confirmed the presence of bioparticles in antigen solutions tested in MAC-ELISA but could not reasonably explain the signal differences observed in MAC-ELISA between VLPs and PPs. Indeed, there are few morphological differences between the two types of particles. This would indicate that the signal difference could be due to the intrinsic antigenic properties of the particles. The self-assembly mode of bioparticle biosynthesis in cells could also explain the differences observed in MAC-ELISA between VLPs and PPs. VLPs are a self-assembly of viral proteins that tend to be as close as possible to the native virus, whereas PPs are structures composed of a backbone of murine leukemia virus (MULV) or human immunodeficiency virus (HIV), pseudotyped with CHIKV envelope proteins. It cannot be excluded that envelope proteins are presented differently depending on the type of bioparticle and that this has an impact on the detection of CHIKV IgM. To verify this hypothesis, analyses of the affinity of specific CHIKV IgM for both VLPs and PPs were evaluated using increasing concentrations of urea. Specific CHIKV IgM seemed to dissociate more easily from VLPs than PPs because a lower urea concentration was able to dissociate the complex. This was confirmed by the slope of the VLPs curve which was higher than that for PPs, indicating a faster dissociation of the VLPs-antibody immunological complex. These results could partially explain the signal difference observed in MAC-ELISA between VLPs and PPs as antigens. To date, there is no study available concerning the comparative affinity of VLPs and PPs for specific antibodies in patient samples.

5. Conclusion

The use of CHIKV bioparticles such as VLPs and PPs represents an attractive alternative to the use of VL, which is traditionally employed in MAC-ELISA. This is primarily due to their innocuity and their ease of production. When used non-purified, PPs give a detection signal higher than for VL, which can help improve the detection sensitivity of MAC-ELISA. The HF5-MALS technology used in this study is a valuable method for characterizing these bioparticles. The results obtained seem to indicate that the remarkable signal obtained with PPs is linked to the viral antigen presentation at the surface of the particles. However, more in-depth experiments are necessary to explore the affinity properties of VLPs and PPs for specific antibodies and to confirm the preliminary results described in the present paper.

Acknowledgments

The authors wish to thank Celine Roesch, Michèle Guillote (Immunoassays department at bioMérieux) for antibody production; Florence Bettsworth, Blandine Le Levreur and Marie-Claire Cavaud (Immunoassays department at bioMérieux) for antibody purification and labeling; Carine Maisse-Paradisi for her welcome and support in the INRA laboratory UMR754. The final manuscript has been red and corrected by RWS life science, Lausanne, CH and Vincent Benoit (Innovation department at bioMérieux)

Ethical approval

All procedures performed in studies involving human participants were in accordance with the ethical standards of the institutional and/or national research committee and with the 1964 Helsinki declaration and its later amendments or comparable ethical standards.

Availability of data and materials

The datasets used and/or analyzed in this work are available from the corresponding author on reasonable request.

Competing interests

All the authors except ILG, DL, CB and PN are employed by bioMérieux SA.

Funding

This study was funded by BioMerieux SA, France and Agence Nationale de la Recherche et de la Technologie, France (G. Theillet's grant CIFRE ID 2015/0514).

Authors' contributions

All of the authors contributed to the study conception. GT, FB performed investigation. GT, FB wrote the original draft and reviewed the manuscript. All of the authors visualized, reviewed, and edited the final manuscript. FB, PD, and ILG performed supervision and funding. TEM investigation was conducted by BC and NP. VLP/PP investigation using HF5-MALS was performed by GT, JM and CS. VLPs and PPs ressources were provided by DL.

Appendix A. Supporting information

Supplementary data associated with this article can be found in the online version at doi:10.1016/j.virol.2019.01.027.

References

Aguado-Martinez, A., Alvarez-Garcia, G., Arnaiz-Seco, I., Innes, E., Ortega-Mora, L., 2005. Use of avidity enzyme-linked immunosorbent assay and avidity Western blot to discriminate between acute and chronic Neospora caninum infection in cattle. J. Vet. Diagn. Investig. 17, 442–450.

Andersson, M., Wittgren, B., Wahlund, K.-G., 2003. Accuracy in multiangle light scattering measurements for molar mass and radius Model calculations and experiments.

Anal. Chem. 75, 4279–4291.
Baklouti, A., Goulet, A., Lichiere, J., Canard, B., Charrel, R.N., Ferron, F., Coutard, B., Papageorgiou, N., 2017. Toscana virus nucleoprotein oligomer organization observed in solution. Acta Crystallogr. Sect. D Struct. Biol. 73, 650–659.
Boura, E., Liebl, D., Spisek, R., Fric, J., Marek, M., Stokrova, J., Holan, V., Forstova, J., 2005. Polyomavirus EGFP-pseudocapsids: analysis of model particles for introduction of proteins and peptides into mammalian cells. FEBS Lett. 579, 6549–6558.
Brouard, C., Bernillon, P., Quatresous, I., Pillonel, J., Assal, A., De Valk, H., Desenclos, J. C., 2008. Estimated risk of Chikungunya viremic blood donation during an epidemic on Reunion Island in the Indian Ocean, 2005 to 2007.
Burt, F.J., Chen, W., Miner, J.J., Lenschow, D.J., Merits, A., Schnettler, E., Kohl, A., Rudd, P.A., Taylor, A., Herrero, L.J., Zaid, A., Ng, L.F., Mahalingam, S., 2017. Chikungunya virus: an update on the biology and pathogenesis of this emerging pathogen. Lancet Infect. Dis.
Chang, L.-J., Dowd, K.A., Mendoza, F.H., Saunders, J.G., Sitar, S., Plummer, S.H., Yamshchikov, G., Sarwar, U.N., Hu, Z., Enama, M.E., 2014. Safety and tolerability of chikungunya virus-like particle vaccine in healthy adults: a phase 1 dose-escalation trial. Lancet 384, 2046–2052.
Cho, B., Jeon, B.Y., Kim, J., Noh, J., Kim, J., Park, M., Park, S., 2008. Expression and evaluation of Chikungunya virus E1 and E2 envelope proteins for serodiagnosis of Chikungunya virus infection. Yonsei Med. J. 49, 828–835.
Chuan, Y.P., Fan, Y.Y., Lua, L., Middelberg, A.P., 2008. Quantitative analysis of virus-like particle size and distribution by field-flow fractionation. Biotechnol. Bioeng. 99, 1425–1433.
Conner, M., Zarley, C., Hu, B., Parsons, S., Drabinski, D., Greiner, S., Smith, R., Jiang, B., Corsaro, B., Madore, H., 1996. Virus-like particles as a rotavirus subunit vaccine. J. Infect. Dis. 174, S88–S92.
Drake, D.M., Keswani, R.K., Pack, D.W., 2010. Effect of serum on transfection by polyethylenimine/virus-like particle hybrid gene delivery vectors. Pharm. Res. 27, 2457–2465.
Fan, C., Ye, X., Ku, Z., Kong, L., Liu, Q., Xu, C., Cong, Y., Huang, Z., 2017. Beta-propiolactone inactivation of coxsackievirus A16 induces structural alteration and surface modification of viral capsids. J. Virol. 91 (e00038-00017).
Fontana, D., Etcheverrigaray, M., Kratje, R., Prieto, C., 2016. Development of rabies virus-like particles for vaccine applications: production, characterization, and protection studies. Methods Mol. Biol. (Clifton N.J.) 1403, 155–166.
Furuya-Kanamori, L., Liang, S., Milinovich, G., Soares Magalhaes, R.J., Clements, A.C., Hu, W., Brasil, P., Frentiu, F.D., Dunning, R., Yakob, L., 2016. Co-distribution and co-infection of chikungunya and dengue viruses. BMC Infect. Dis. 16, 84.
Gonzaga, H.T., Ribeiro, V.S., Feliciano, N.D., Manhani, M.N., Silva, D.A., Ueta, M.T., Costa-Cruz, J.M., 2011. IgG avidity in differential serodiagnosis of human strongyloidiasis active infection. Immunol. Lett. 139, 87–92.
Hammon, W., Rudnick, A., Sather, G.E., 1960. Viruses associated with epidemic hemorrhagic fevers of the Philippines and Thailand.
Huglin MB, M.B., 1972. Light Scattering From Polymer Solutions. Academic Press, UK, pp. 165–331.
Jose, J., Snyder, J.E., Kuhn, R.J., 2009. A structural and functional perspective of alphavirus replication and assembly. Future Microbiol. 4, 837–856.
Khan, M., Dhanwani, R., Kumar, J.S., Rao, P.V., Parida, M., 2014. Comparative evaluation of the diagnostic potential of recombinant envelope proteins and native cell culture purified viral antigens of Chikungunya virus. J. Med. Virol. 86, 1169–1175.
Koutsky, L.A., Ault, K.A., Wheeler, C.M., Brown, D.R., Barr, E., Alvarez, F.B., Chiacchierini, L.M., Jansen, K.U., 2002. A controlled trial of a human papillomavirus type 16 vaccine. New Engl. J. Med. 347, 1645–1651.
Kushnir, N., Streatfield, S.J., Yusibov, V., 2012. Virus-like particles as a highly efficient vaccine platform: diversity of targets and production systems and advances in clinical development. Vaccine 31, 58–83.
Lamounier, T.A., de Oliveira, L.M., de Camargo, B.R., Rodrigues, K.B., Noronha, E.F., Ribeiro, B.M., Nagata, T., 2015. Production of Brazilian human norovirus VLPs and comparison of purification methods. Braz. J. Microbiol 46, 1265–1268.
Li, J., Zhang, Q., Zhang, S., Li, C., Liu, Q., Liang, M., Li, D., 2014. Virus-like particle-based immunoglobulin M capture enzyme-linked immunosorbent assay for the detection of IgM antibodies against Chikungunya virus. Bing. Du Xue Bao= Chin. J. Virol. 30, 599–604.
Lumsden, W.H., 1955. An epidemic of virus disease in Southern Province, Tanganyika Territory, in 1952–1953. II. Gen. Descr. Epidemiol.
Martin, D.A., Muth, D.A., Brown, T., Johnson, A.J., Karabatsos, N., Roehrig, J.T., 2000. Standardization of immunoglobulin M capture enzyme-linked immunosorbent assays for routine diagnosis of arboviral infections. J. Clin. Microbiol. 38, 1823–1826.
McFee, R.B., 2018. Selected mosquito-borne illnesses—Chikungunya. Dis.-a-Mon.
Metz, S.W., Gardner, J., Geertsema, C., Le, T.T., Goh, L., Vlak, J.M., Suhrbier, A., Pijlman, G.P., 2013. Effective chikungunya virus-like particle vaccine produced in insect cells. PLoS Negl. Trop. Dis. 7, e2124.
Metz, S.W., Pijlman, G.P., 2016. Production of Chikungunya Virus-Like Particles and Subunit Vaccines in Insect Cells, Chikungunya Virus. Springer, pp. 297–309.
Minder, E.I., Schibli, A., Mahrer, D., Nesic, P., Plüer, K., 2011. Effects of different centrifugation conditions on clinical chemistry and Immunology test results. BMC Clin. Pathol. 11, 6.
Mishra, B., Sharma, M., Pujhari, S.K., Ratho, R.K., Gopal, D.S., Kumar, C.N., Sarangi, G., Chayani, N., Varma, S.C., 2011. Utility of multiplex reverse transcriptase-polymerase chain reaction for diagnosis and serotypic characterization of dengue and chikungunya viruses in clinical samples. Diagn. Microbiol. Infect. Dis. 71, 118–125.
Mishra, N., Caciula, A., Price, A., Thakkar, R., Ng, J., Chauhan, L.V., Jain, K., Che, X., Espinosa, D.A., Montoya Cruz, M., Balmaseda, A., Sullivan, E.H., Patel, J.J., Jarman, R.G., Rakeman, J.L., Egan, C.T., Reusken, C., Koopmans, M.P.G., Harris, E., Tokarz, R., Briese, T., Lipkin, W.I., 2018. Diagnosis of zika virus infection by peptide array and enzyme-linked immunosorbent assay. mBio 9.
Noranate, N., Takeda, N., Chetanachan, P., Sittisaman, P., Nuegoonpipat, A., Anantapreecha, S., 2014. Characterization of chikungunya virus-like particles. PLoS One 9, e108169.
Pattenden, L.K., Middelberg, A.P., Niebert, M., Lipin, D.I., 2005. Towards the preparative and large-scale precision manufacture of virus-like particles. Trends Biotechnol. 23, 523–529.
Pease 3rd, L.F., Lipin, D.I., Tsai, D.H., Zachariah, M.R., Lua, L.H., Tarlov, M.J., Middelberg, A.P., 2009. Quantitative characterization of virus-like particles by asymmetrical flow field flow fractionation, electrospray differential mobility analysis, and transmission electron microscopy. Biotechnol. Bioeng. 102, 845–855.
Perrin, P., Morgeaux, S., 1995. Inactivation of DNA by beta-propiolactone. Biol.: J. Int. Assoc. Biol. Stand. 23, 207–211.
Peyrefitte, C.N., Pastorino, B.A., Bessaud, M., Gravier, P., Tock, F., Couissinier-Paris, P., Martial, J., Huc-Anais, P., Césaire, R., Grandadam, M., 2005. Dengue type 3 virus, Saint Martin, 2003–2004. Emerg. Infect. Dis. 11, 757.
Peyret, H., 2015. A protocol for the gentle purification of virus-like particles produced in plants. J. Virol. Methods 225, 59–63.
Podzimek, S., 2011. Light Scattering, Size Exclusion Chromatography and Asymmetric Flow Field Flow Fractionation: Powerful Tools for the Characterization of Polymers, Proteins and Nanoparticles. John Wiley & Sons.
Priya, R., Khan, M., Rao, M.K., Parida, M., 2014. Cloning, expression and evaluation of diagnostic potential of recombinant capsid protein based IgM ELISA for chikungunya virus. J. Virol. Methods 203, 15–22.
Pushko, P., Tumpey, T.M., Bu, F., Knell, J., Robinson, R., Smith, G., 2005. Influenza virus-like particles comprised of the HA, NA, and M1 proteins of H9N2 influenza virus induce protective immune responses in BALB/c mice. Vaccine 23, 5751–5759.
Qureshi, R.N., Kok, W.T., 2011. Application of flow field-flow fractionation for the characterization of macromolecules of biological interest: a review. Anal. Bioanal. Chem. 399, 1401–1411.
Rathore, M.H., Runyon, J., Haque, T.U., 2017. Emerging Infectious Diseases.
Robinson, M.C., 1955. An epidemic of virus disease in Southern Province, Tanganyika Territory, in 1952-53. I. Clin. Features.
Rougeron, V., Sam, I.C., Caron, M., Nkoghe, D., Leroy, E., Roques, P., 2015. Chikungunya, a paradigm of neglected tropical disease that emerged to be a new health global risk. J. Clin. Virol.: Off. Publ. Pan Am. Soc. Clin. Virol. 64, 144–152.
Saraswat, S., Athmaram, T., Parida, M., Agarwal, A., Saha, A., Dash, P.K., 2016. Expression and characterization of yeast derived Chikungunya virus like particles (CHIK-VLPs) and its evaluation as a potential vaccine candidate. PLoS Negl. Trop. Dis. 10, e0004782.
Schwameis, M., Buchtele, N., Wadowski, P.P., Schoergenhofer, C., Jilma, B., 2016. Chikungunya vaccines in development. Hum. Vaccin. Immunother. 12, 716–731.
Schwartz, O., Albert, M.L., 2010. Biology and pathogenesis of chikungunya virus. Nat. Rev. Microbiol. 8, 491–500.
Scolnick, E.M., McLean, A.A., West, D.J., McAleer, W.J., Miller, W.J., Buynak, E.B., 1984. Clinical evaluation in healthy adults of a hepatitis B vaccine made by recombinant DNA. JAMA 251, 2812–2815.
Smolander, H., Koskinen, J.O., Vainionpää, R., Meltola, N.J., Lappalainen, M., Hedman, K., Soini, A.E., 2010. A novel antibody avidity methodology for rapid point-of-care serological diagnosis. J. Virol. Methods 166, 86–91.
Urakami, A., Sakurai, A., Ishikawa, M., Yap, M.L., Flores-Garcia, Y., Haseda, Y., Aoshi, T., Zavala, F.P., Rossmann, M.G., Kuno, S., Ueno, R., Akahata, W., 2017. Development of a novel virus-like particle vaccine platform that mimics the immature form of alphavirus. Clin. Vaccin. Immunol. 24.
Wagner, M., Holzschuh, S., Traeger, A., Fahr, A., Schubert, U.S., 2014. Asymmetric flow field-flow fractionation in the field of nanomedicine. Anal. Chem. 86, 5201–5210.
Wu, J., Zhao, C., Liu, Q., Huang, W., Wang, Y., 2017. Development and application of a bioluminescent imaging mouse model for Chikungunya virus based on pseudovirus system. Vaccine 35, 6387–6394.
Yap, G., Pok, K.Y., Lai, Y.L., Hapuarachchi, H.C., Chow, A., Leo, Y.S., Tan, L.K., Ng, L.C., 2010. Evaluation of Chikungunya diagnostic assays: differences in sensitivity of serology assays in two independent outbreaks. PLoS Negl. Trop. Dis. 4, e753.
Yohannes, G., Jussila, M., Hartonen, K., Riekkola, M.L., 2011. Asymmetrical flow field-flow fractionation technique for separation and characterization of biopolymers and bioparticles. J. Chromatogr. A 1218, 4104–4116.